
This copy is for your personal, non-commercial use only.

If you wish to distribute this article to others, you can order high-quality copies for your colleagues, clients, or customers by [clicking here](#).

Permission to republish or repurpose articles or portions of articles can be obtained by following the guidelines [here](#).

The following resources related to this article are available online at www.sciencemag.org (this information is current as of March 3, 2011):

Updated information and services, including high-resolution figures, can be found in the online version of this article at:

<http://www.sciencemag.org/content/331/6021/1199.full.html>

Supporting Online Material can be found at:

<http://www.sciencemag.org/content/suppl/2011/01/19/science.1200609.DC1.html>

This article **cites 27 articles**, 12 of which can be accessed free:

<http://www.sciencemag.org/content/331/6021/1199.full.html#ref-list-1>

This article has been **cited by** 1 articles hosted by HighWire Press; see:

<http://www.sciencemag.org/content/331/6021/1199.full.html#related-urls>

This article appears in the following **subject collections**:

Medicine, Diseases

<http://www.sciencemag.org/cgi/collection/medicine>

coil domain in the crystal structure would need to be at an angle to better fit the EM density. This could be accommodated by some flexibility between the head domains and the coiled-coil domain of SAS-6. Allowing for this flexibility, we modeled ring assemblies containing 6 to 12 SAS-6 dimers (Fig. 4C). Compared with the N-SAS-6¹⁻¹⁷⁹ F131D crystal structure, the eight- and ninefold symmetric rings required the smallest changes in the orientation of the head domains. With their radially projecting, stalklike coiled-coil domains, these ring assemblies resemble centriolar cartwheels. The inner diameter of the modeled ninefold symmetric ring was comparable to the diameter of the cartwheel hubs observed in procentrioles by cryo-electron tomography (200 Å) (32). Consistent with our ring models with projecting coiled-coil domains, the C-termini of SAS-6 in *Chlamydomonas* are found in the outer regions of the centriolar cartwheel spokes (fig. S10).

No cartwheel has been identified so far in *Caenorhabditis elegans*. Instead, a central centriolar tube was found, whose presence requires SAS-6 (33). This alternative assembly could be due to structural differences in SAS-6, as motif II in *C. elegans* and *C. briggsae* is very distinct from the other SAS-6 homologs [fig. S2 and (28)].

We suggest that SAS-6 self-assembly is a contributing factor in the structural organization of centriolar cartwheels cores. However, our data also suggest that other centriolar components are probably needed for a faithful and stable ninefold symmetric SAS-6 assembly in vivo. This notion is in agreement with the presence of alternative SAS-6 assemblies that are observed when SAS-6 is overexpressed in *Drosophila* (14, 34).

References and Notes

- M. Bettencourt-Dias, D. M. Glover, *Nat. Rev. Mol. Cell Biol.* **8**, 451 (2007).
- E. A. Nigg, J. W. Raff, *Cell* **139**, 663 (2009).
- P. Strnad, P. Gönczy, *Trends Cell Biol.* **18**, 389 (2008).
- J. Loncarek, A. Khodjakov, *Mol. Cells* **27**, 135 (2009).
- T. Cavalier-Smith, *J. Cell Sci.* **16**, 529 (1974).
- R. D. Allen, *J. Cell Biol.* **40**, 716 (1969).
- R. G. Anderson, R. M. Brenner, *J. Cell Biol.* **50**, 10 (1971).
- K. Matsuura, P. A. Lefebvre, R. Kamiya, M. Hirono, *J. Cell Biol.* **165**, 663 (2004).
- M. Hiraki, Y. Nakazawa, R. Kamiya, M. Hirono, *Curr. Biol.* **17**, 1778 (2007).
- M. Jerka-Dziadosz et al., *Cytoskeleton (Hoboken)* **67**, 161 (2010).
- J. Kleylein-Sohn et al., *Dev. Cell* **13**, 190 (2007).
- Y. Nakazawa, M. Hiraki, R. Kamiya, M. Hirono, *Curr. Biol.* **17**, 2169 (2007).
- B. P. Culver, J. B. Meehl, T. H. Giddings Jr., M. Winey, *Mol. Biol. Cell* **20**, 1865 (2009).
- A. Rodrigues-Martins et al., *Curr. Biol.* **17**, 1465 (2007).
- E. K. Vadar, T. Stearns, *J. Cell Biol.* **178**, 31 (2007).
- A. Rodrigues-Martins, M. Riparbelli, G. Callaini, D. M. Glover, M. Bettencourt-Dias, *Science* **316**, 1046 (2007); 10.1126/science.1142950.
- A. Dammermann et al., *Dev. Cell* **7**, 815 (2004).
- S. Leidel, M. Delattre, L. Cerutti, K. Baumer, P. Gönczy, *Nat. Cell Biol.* **7**, 115 (2005).
- T. Yabe, X. Ge, F. Pelegri, *Dev. Biol.* **312**, 44 (2007).
- R. Hagedanck, Y. D. Stierhof, C. J. Wilkinson, E. A. Nigg, *Nat. Cell Biol.* **7**, 1140 (2005).
- P. Strnad et al., *Dev. Cell* **13**, 203 (2007).
- J. Dobbelaere et al., *PLoS Biol.* **6**, e224 (2008).
- Materials and methods are available as supporting material on Science Online.
- Y. Li et al., *EMBO J.* **27**, 290 (2008).
- S. N. Andres, M. Modesti, C. J. Tsai, G. Chu, M. S. Junop, *Mol. Cell* **28**, 1093 (2007).
- M. S. Junop et al., *EMBO J.* **19**, 5962 (2000).
- B. L. Sibanda et al., *Nat. Struct. Biol.* **8**, 1015 (2001).
- Z. Carvalho-Santos et al., *J. Cell Sci.* **123**, 1414 (2010).
- Single-letter abbreviations for the amino acid residues are as follows: A, Ala; C, Cys; D, Asp; E, Glu; F, Phe; G, Gly; H, His; I, Ile; K, Lys; L, Leu; M, Met; N, Asn; P, Pro; Q, Gln; R, Arg; S, Ser; T, Thr; V, Val; W, Trp; and Y, Tyr.
- E. Krissinel, K. Henrick, *J. Mol. Biol.* **372**, 774 (2007).
- L. Lo Conte, C. Chothia, J. Janin, *J. Mol. Biol.* **285**, 2177 (1999).
- P. Guichard, D. Chrétien, S. Marco, A. M. Tassin, *EMBO J.* **29**, 1565 (2010).
- L. Pelletier, E. O'Toole, A. Schwager, A. A. Hyman, T. Müller-Reichert, *Nature* **444**, 619 (2006).
- J. Gopalakrishnan et al., *J. Biol. Chem.* **285**, 8759 (2010).
- F. Glaser et al., *Bioinformatics* **19**, 163 (2003).
- A. K. Gillingham, S. Munro, *EMBO Rep.* **1**, 524 (2000).
- The structure factors and coordinates of *D. rerio* N-SAS-6¹⁻¹⁵⁶ and *D. rerio* N-SAS-6¹⁻¹⁷⁹ F131D have been deposited at the Protein Data Bank Europe under wwPDB ID codes 2y3v and 2y3w. We gratefully acknowledge P. Evans (MRC-LMB, Cambridge, UK) for his modeling of SAS-6 ring assemblies and our beamline support team, M. Nanao at ID29 and H. Belrhali at BM14UK at the European Synchrotron Radiation Facility (Grenoble, France). We thank L. Rey (MRC-LMB) for the kind gift of U2OS cells and S. Munro (MRC-LMB) for the kind gift of a construct expressing the red fluorescent protein (RFP)-tagged C-terminal PACT domain of pericentrin. This work was supported by a MRC Career Development Fellowship (to M.v.B.); Grants-in-Aid for Scientific Research from the Ministry of Education, Culture, Science and Technology of Japan (21370088) (to M.H.); and a European Molecular Biology Organization long-term fellowship (to B.Z.). Material will be provided to academic and not-for-profit research organizations under the MRC's standard academic Material Transfer Agreement. The UltraSpin software will be provided by MRC under an academic license.

Supporting Online Material

www.sciencemag.org/cgi/content/full/science.1199325/DC1
Materials and Methods
Figs. S1 to S10
Tables S1 and S2
References

20 October 2010; accepted 19 January 2011
Published online 27 January 2011;
10.1126/science.1199325

DAXX/ATRX, MEN1, and mTOR Pathway Genes Are Frequently Altered in Pancreatic Neuroendocrine Tumors

Yuchen Jiao,^{1*} Chanjuan Shi,^{2*} Barish H. Edil,³ Roeland F. de Wilde,² David S. Klimstra,⁴ Anirban Maitra,⁵ Richard D. Schulick,³ Laura H. Tang,⁴ Christopher L. Wolfgang,³ Michael A. Choti,³ Victor E. Velculescu,¹ Luis A. Diaz Jr.,^{1,6} Bert Vogelstein,¹ Kenneth W. Kinzler,^{1†} Ralph H. Hruban,^{5†} Nickolas Papadopoulos^{1†}

Pancreatic neuroendocrine tumors (PanNETs) are a rare but clinically important form of pancreatic neoplasia. To explore the genetic basis of PanNETs, we determined the exomic sequences of 10 nonfamilial PanNETs and then screened the most commonly mutated genes in 58 additional PanNETs. The most frequently mutated genes specify proteins implicated in chromatin remodeling: 44% of the tumors had somatic inactivating mutations in *MEN1*, which encodes menin, a component of a histone methyltransferase complex, and 43% had mutations in genes encoding either of the two subunits of a transcription/chromatin remodeling complex consisting of DAXX (death-domain-associated protein) and ATRX (α thalassemia/mental retardation syndrome X-linked). Clinically, mutations in the *MEN1* and *DAXX/ATRX* genes were associated with better prognosis. We also found mutations in genes in the mTOR (mammalian target of rapamycin) pathway in 14% of the tumors, a finding that could potentially be used to stratify patients for treatment with mTOR inhibitors.

Pancreatic neuroendocrine tumors (PanNETs) are the second-most common malignancy of the pancreas. The 10-year survival rate

of patients with PanNETs is only 40% (1–3). PanNETs are usually sporadic but can arise in multiple endocrine neoplasia type 1 and more

rarely in other syndromes, including von Hippel-Lindau (VHL) syndrome and tuberous sclerosis (4). “Functional” PanNETs secrete hormones that cause systemic effects, whereas “nonfunctional” PanNETs do not and therefore cannot always be readily distinguished from other neoplasms of the pancreas. Nonfunctional PanNETs grow silently, and patients often present with either an asymptomatic abdominal mass or symptoms of abdominal pain secondary to compression by a large tumor. Surgical resection is the treatment of choice, but many patients present with unresect-

¹Ludwig Center for Cancer Genetics and Howard Hughes Medical Institutions, Johns Hopkins Kimmel Cancer Center, Baltimore, MD 21231, USA. ²Department of Pathology, Sol Goldman Pancreatic Cancer Research Center, Johns Hopkins Medical Institutions, Baltimore, MD 21231, USA. ³Department of Surgery, Sol Goldman Pancreatic Cancer Research Center, Johns Hopkins Medical Institutions, Baltimore, MD 21231, USA. ⁴Department of Pathology, Memorial Sloan-Kettering Cancer Center, New York, NY 10065, USA. ⁵Departments of Pathology and Oncology, Sol Goldman Pancreatic Cancer Research Center, Johns Hopkins Medical Institutions, Baltimore, MD 21231, USA. ⁶Swim Across America Laboratory, Johns Hopkins University, Baltimore, MD 21231, USA.

*These authors contributed equally to this work.

†To whom correspondence should be addressed. E-mail: npapado1@jhmi.edu (N.P.); rhruban@jhmi.edu (R.H.H.); kinzke@jhmi.edu (K.W.K.)

able tumors or extensive metastatic disease, and medical therapies are relatively ineffective in these cases.

There is currently insufficient information about this tumor to either predict prognosis of patients diagnosed with PanNETs or to develop companion diagnostics and personalized treatments to improve disease management. Biallelic inactivation of the *MEN1* gene, usually through a mutation in one allele coupled with

loss of the remaining wild-type allele, occurs in 25 to 30% of PanNETs (5, 6). *MEN1* is a tumor suppressor gene that, when mutated in the germline, predisposes to multiple endocrine neoplasia type 1 syndrome. Chromosomal gains and losses and expression analyses have revealed candidate loci for genes involved in the development of PanNETs, but these have not been substantiated through genetic or functional analyses (7–9).

To gain insights into the genetic basis of this tumor type, we determined the exomic sequence of ~18,000 protein-coding genes in a discovery set of 10 well-characterized sporadic PanNETs. A clinically homogeneous set of tumors of high neoplastic cellularity is essential for the successful identification of genes and pathways involved in any tumor type. Thus, we excluded small-cell and large-cell neuroendocrine carcinomas and studied only samples that were not part of a familial syndrome associated with PanNETs (table S1) (1). We microdissected tumor samples in order to achieve a neoplastic cellularity of >80%. DNA from the enriched neoplastic

samples and from matched non-neoplastic tissue from 10 patients was used to prepare fragment libraries suitable for massively parallel sequencing. The coding sequences were enriched by capture with the SureSelect Enrichment System and sequenced by use of an Illumina GAIIX platform (10). The average coverage of each base in the targeted regions was 101-fold, and 94.8% of the bases were represented by at least 10 reads (table S2).

We identified 157 somatic mutations in 149 genes among the 10 tumors used in the discovery set. The mutations per tumor ranged from 8 to 23, with a mean of 16 (table S3). Of these mutations, 91% were validated by means of Sanger sequencing. There were some obvious differences between the genetic landscapes of PanNETs and those of pancreatic ductal adenocarcinomas (PDAC) (11). First, there were 60% fewer genes mutated per tumor in PanNETs than in PDACs. Second, the genes most commonly affected by mutation in PDACs (*KRAS*, *TGF-β* pathway, *CDKN2A*, and *TP53*) were rarely altered in PanNETs and vice versa (Table 1). Third, the

Table 1. Comparison of commonly mutated genes in PanNETs and PDAC based on 68 PanNETs and 114 PDACs.

Genes*	PanNET	PDAC†
<i>MEN1</i>	44%	0%
<i>DAXX</i> , <i>ATRX</i>	43%	0%
Genes in mTOR pathway	15%	0.80%
<i>TP53</i>	3%	85%
<i>KRAS</i>	0%	100%
<i>CDKN2A</i>	0%	25%
<i>TGFBRI1</i> , <i>SMAD3</i> , <i>SMAD4</i>	0%	38%

Table 2. Mutations in *MEN1*, *DAXX*, *ATRX*, *PTEN*, *TSC2*, *PIK3CA*, and *TP53* in human PanNETs. (hom) indicates these mutations appear homozygous.

Sample*	Gene	Transcript accession	Nucleotide (genomic)†	Nucleotide (cDNA)	Amino acid (protein)‡	Mutation type
PanNET3PT	<i>ATRX</i>	CCDS14434.1	g.chrX:76716462G>A (hom)	c.6235C>T(hom)	p.R2079X	Nonsense
PanNET5PT	<i>ATRX</i>	CCDS14434.1	g.chrX:76742636G>A	c.5620C>T	p.Q1874X	Nonsense
PanNET13PT	<i>ATRX</i>	CCDS14434.1	g.chrX:76741560delA	c.5932delT	fs	Indel
PanNET27PT	<i>ATRX</i>	CCDS14434.1	g.chrX:76700959_76700962delATAA	c.6338_6341delTTAT	fs	Indel
PanNET35PT	<i>ATRX</i>	CCDS14434.1	g.chrX:76806893_76806909delAA TTTCTTCTAAAAGCA	c.3824_3840delTGT CTTTTAGAAGAAATT	fs	Indel
PanNET52PT	<i>ATRX</i>	CCDS14434.1	g.chrX:76796337_76796340delCTTT	c.4221_4224delAAAG	fs	Indel
PanNET59PT	<i>ATRX</i>	CCDS14434.1	g.chrX:76761014C>A	c.5364G>T	p.Q1788H	Missense
PanNET78PT	<i>ATRX</i>	CCDS14434.1	g.chrX:76665406C>T	c.6829G>A	p.E2277K	Missense
PanNET85PT	<i>ATRX</i>	CCDS14434.1	g.chrX:76794404dupC	c.4414dupG	fs	Indel
PanNET98PT	<i>ATRX</i>	CCDS14434.1	g.chrX:76700832T>A(hom)	c.6468A>T(hom)	p.Q2156H	Missense
PanNET100PT	<i>ATRX</i>	CCDS14434.1	g.chrX:76762518_76762521 delCACT(hom)	c.5270_5272delAGTG(hom)	fs	Indel
PanNET112PT	<i>ATRX</i>	CCDS14434.1	g.chrX:76826041T>A(hom)	c.1363A>T(hom)	p.K455X	Nonsense
PanNET25PT	<i>DAXX</i>	CCDS4776.1	g.chr6:33394939delT	c.1976delA	fs	Indel
PanNET31PT	<i>DAXX</i>	CCDS4776.1	g.chr6:33394935delC(hom)	c.1980delG(hom)	fs	Indel
PanNET44PT	<i>DAXX</i>	CCDS4776.1	g.chr6:33394795delG	c.2120delC	fs	Indel
PanNET56PT	<i>DAXX</i>	CCDS4776.1	g.chr6:33397319delG	c.211delC	fs	Indel
PanNET77PT	<i>DAXX</i>	CCDS4776.1	g.chr6:33396614G>A	c.916C>T	p.R306X	Nonsense
PanNET84PT	<i>DAXX</i>	CCDS4776.1	g.chr6:33395309delG	c.1766delC	fs	Indel
PanNET87PT	<i>DAXX</i>	CCDS4776.1	g.chr6:33397141A>C	c.389T>G	p.L130R	Missense
PanNET93PT	<i>DAXX</i>	CCDS4776.1	g.chr6:33396641C>G	c.889G>C	p.A297P	Missense
PanNET94PT	<i>DAXX</i>	CCDS4776.1	g.chr6:33394872_33394873insA	c.2042_2043insT	fs	Indel
PanNET95PT	<i>DAXX</i>	CCDS4776.1	g.chr6:33397221_33397224delCGCC	c.306_309delGGCG	fs	Indel
PanNET96PT	<i>DAXX</i>	CCDS4776.1	g.chr6:33396167delC	c.1219delG	fs	Indel
PanNET97PT	<i>DAXX</i>	CCDS4776.1	g.chr6:33395838C>A(hom)	c.1393G>T(hom)	p.E465X	Nonsense
PanNET102PT	<i>DAXX</i>	CCDS4776.1	g.chr6:33397515T>A	c.166A>T	p.K56X	Nonsense
PanNET103PT	<i>DAXX</i>	CCDS4776.1	g.chr6:33397579delA	c.102delT	fs	Indel
PanNET104PT	<i>DAXX</i>	CCDS4776.1	g.chr6:33396604_33396605insACT(hom)	c.925_926insAGT(hom)	p.L309QF	Indel/missense
PanNET108PT	<i>DAXX</i>	CCDS4776.1	g.chr6:33395828delT(hom)	c.1403delA(hom)	fs	Indel
PanNET133PT	<i>DAXX</i>	CCDS4776.1	g.chr6:33395889C>A(hom)	c.1342G>T(hom)	p.E448X	Nonsense
PanNET3PT	<i>MEN1</i>	CCDS8083.1	g.chr11:64331709C>A(hom)	c.689G>T(hom)	p.G230V	Missense
PanNET5PT	<i>MEN1</i>	CCDS8083.1	g.chr11:64332046A>G(hom)	c.562T>C(hom)	p.W188R	Missense
PanNET6PT	<i>MEN1</i>	CCDS8083.1	g.chr11:64333812_64333828delCA CGGCTGGAGACACCC	c.329_345delGGG TGTTCTCAGCCGTG	fs	Indel

continued on next page

Sample*	Gene	Transcript accession	Nucleotide (genomic)†	Nucleotide (cDNA)	Amino acid (protein)‡	Mutation type
PanNET10PT	<i>MEN1</i>	CCDS8083.1	g.chr11:64334105_64334108 delTCGT(hom)	c.50_53delACGA(hom)	fs	Indel
PanNET23PT	<i>MEN1</i>	CCDS8083.1	g.chr11:64331233_64331234delAG(hom)	c.832_833delCT(hom)	fs	Indel
PanNET29PT	<i>MEN1</i>	CCDS8083.1	g.chr11:64334070C>A(hom)	c.88G>T(hom)	p.E30X	Nonsense
PanNET31PT	<i>MEN1</i>	CCDS8083.1	g.chr11:64328587G>T	c.1643C>A	p.S548X	Nonsense
PanNET39PT	<i>MEN1</i>	CCDS8083.1	g.chr11:64333993_64333999 delAGGGATG(hom)	c.159_165delCATCCCT(hom)	fs	Indel
PanNET44PT	<i>MEN1</i>	CCDS8083.1	g.chr11:64333955delG	c.203delC	fs	Indel
PanNET45PT	<i>MEN1</i>	CCDS8083.1	g.chr11:64330370G>C	c.974C>G	p.P325R	Missense
PanNET52PT	<i>MEN1</i>	CCDS8083.1	g.chr11:64333876delG	c.282delC	fs	Indel
PanNET57PT	<i>MEN1</i>	CCDS8083.1	g.chr11:64334002delG(hom)	c.156delC(hom)	fs	Indel
PanNET59PT	<i>MEN1</i>	CCDS8083.1	g.chr11:64329234G>A	c.1213C>T	p.Q405X	Nonsense
PanNET61PT	<i>MEN1</i>	CCDS8083.1	g.chr11:64334049_64334201delG GAGCACCAGTCC GGCTCCTCTCGGCC CAGCTCGGCAGCAAA CAGGGCGACCACGTCGTCGA TGGAGCGCAGCGGGAA CAGCGTCTTCTGGGCGGCC TTCAGCCCCATGGCGGCGGCGG TGGGCGGCGGCCTG CAAGGCAAGCCGGGGAG(hom)	c.1_109delAT GGGGCTGAAGCCCG CCCAGAAGACGCTGTT CCCCTGCGCTCCATCGAC GACGTGGTGCGCCTGTTTG CTGCCGAGC TGGGCCGAGAGGA GCCGGACCTGGTGCTCC(hom)	fs	Indel
PanNET64PT	<i>MEN1</i>	CCDS8083.1	g.chr11:64333781delC	c.377delG	fs	Indel
PanNET69PT	<i>MEN1</i>	CCDS8083.1	g.chr11:64330291delA	c.1053delT	fs	Indel
PanNET77PT	<i>MEN1</i>	CCDS8083.1	g.chr11:64334063_64334079delGG CTCCTCTCGGCCAG	c.79_95delCT GGGCCGAGAGGAGCC	fs	Indel
PanNET78PT	<i>MEN1</i>	CCDS8083.1	g.chr11:64332045C>T	c.563G>A	p.W188X	Nonsense
PanNET83PT	<i>MEN1</i>	CCDS8083.1	g.chr11:64330369delG	c.975delC	fs	Indel
PanNET84PT	<i>MEN1</i>	CCDS8083.1	g.chr11:64334139G>A	c.19C>T	p.Q7X	Nonsense
PanNET85PT	<i>MEN1</i>	CCDS8083.1	g.chr11:64332011_64332012insCTGT	c.596_597insACAG	fs	Indel
PanNET93PT	<i>MEN1</i>	CCDS8083.1	g.chr11:64333906_64333909delAGAC	c.249_252delGTCT	fs	Indel
PanNET94PT	<i>MEN1</i>	CCDS8083.1	g.chr11:64333906_64333909delAGAC	c.249_252delGTCT	fs	Indel
PanNET95PT	<i>MEN1</i>	CCDS8083.1	g.chr11:64332032delC(hom)	c.576delG(hom)	fs	Indel
PanNET96PT	<i>MEN1</i>	CCDS8083.1	g.chr11:64331269T>C	c.IVS799-2A>G	c.IVS799-2A>G	Splice site
PanNET99PT	<i>MEN1</i>	CCDS8083.1	g.chr11:64331938C>A	c.IVS669+1G>T	c.IVS669+1G>T	Splice site
PanNET100PT	<i>MEN1</i>	CCDS8083.1	g.chr11:64331940_64331941delCG(hom)	c.667_668delCG(hom)	fs	Indel
PanNET102PT	<i>MEN1</i>	CCDS8083.1	g.chr11:64332102G>A	c.506C>T	p.A169V	Missense
PanNET108PT	<i>MEN1</i>	CCDS8083.1	g.chr11:64331200_64331251delG CAGCCTGGCCAC TTCCCTCTACTGACCTTT CCAGATGTCCCAGGTCATAGA(hom)	c.815_837delTTC TATGACCTGGGA CATCTGGAA(hom)	del exon and intron	Indel
PanNET109PT	<i>MEN1</i>	CCDS8083.1	g.chr11:64334093A>C	c.65T>G	p.L22R	Missense
PanNET10PT	<i>PIK3CA</i>	CCDS43171.1	g.chr3:180418785G>A	c.1633G>A	p.E545K	Missense
PanNET10PT	<i>PTEN</i>	CCDS31238.1	g.chr10:89707693delG	c.738delG	fs	Indel
PanNET31PT	<i>PTEN</i>	CCDS31238.1	g.chr10:89682819T>G	c.323T>G	p.L108R	Missense
PanNET29PT	<i>PTEN</i>	CCDS31238.1	g.chr10:89710790_89710791ins TGACAAGGAATAT CTAGTACTACTTTAA	c.961_962insTGA CAAGGAATATCTAG TACTTACTTTAA	fs	Indel
PanNET96PT	<i>PTEN</i>	CCDS31238.1	g.chr10:89675287T>C(hom)	c.202T>C(hom)	p.Y68H	Missense
PanNET104PT	<i>PTEN</i>	CCDS31238.1	g.chr10:89701856G>A(hom)	c.494G>A(hom)	p.G165E	Missense
PanNET24PT	<i>TP53</i>	CCDS11118.1	g.chr17:7518284G>A	c.722C>T	p.S241F	Missense
PanNET91PT	<i>TP53</i>	CCDS11118.1	g.chr17:7519210delA(hom)	c.445delT(hom)	fs	Indel
PanNET100PT	<i>TP53</i>	CCDS11118.1	g.chr17:7520101delT(hom)	c.311delA(hom)	fs	Indel
PanNET2PT	<i>TSC2</i>	CCDS10458.1	g.chr16:2070191C>T	c.3422C>T	p.A1141V	Missense
PanNET31PT	<i>TSC2</i>	CCDS10458.1	g.chr16:2074957G>A	c.4498G>A	p.V1500M	Missense
PanNET44PT	<i>TSC2</i>	CCDS10458.1	g.chr16:2074337_2074338delTG	c.4113_4114delTG	fs	Indel
PanNET70PT	<i>TSC2</i>	CCDS10458.1	g.chr16:2078571C>T	c.5383C>T	p.R1795C	Missense
PanNET93PT	<i>TSC2</i>	CCDS10458.1	g.chr16:2038643C>A	c.26C>A	p.S9X	Nonsense
PanNET112PT	<i>TSC2</i>	CCDS10458.1	g.chr16:2076836A>G	c.4952A>G	p.N1651S	Missense

*Samples PanNET3, PanNET7, PanNET10, PanNET21, PanNET23, PanNET24, PanNET25, PanNET31, PanNET36, and PanNET93 were used for the initial (discovery set) screen. †Coordinates refer to human reference genome hg18 release (NCBI 36.1, March 2006). ‡Single-letter abbreviations for the amino acid residues are as follows: A, Ala; C, Cys; D, Asp; E, Glu; F, Phe; G, Gly; H, His; I, Ile; K, Lys; L, Leu; M, Met; N, Asn; P, Pro; Q, Gln; R, Arg; S, Ser; T, Thr; V, Val; W, Trp; and Y, Tyr.

spectrum of mutations in PDAC and PanNET were different, with C-to-T transitions more common in PDACs than in PanNETs and C-to-G transversions more common in PanNETs than in PDACs (table S4). This suggests that mutations in PanNETs and PDAC arise through different mechanisms, perhaps because of exposure to different environmental carcinogens or through the action of different DNA-repair pathways.

We next selected genes for further analysis that were well-documented components of a pathway that was genetically altered in more than one tumor because alterations in these genes are most likely to be clinically relevant. Four genes were mutated in at least two tumors in the discovery set: *MEN1* in five, *DAXX* in three, *PTEN* in two, and *TSC2* in two. *ATRX* was mutated in only one sample in the discovery set, but its product forms a heterodimer with *DAXX* and, therefore, is part of the same pathway, so it was also evaluated in the validation set. Similarly, *PIK3CA* was included because its product is part of the mammalian target of rapamycin (mTOR) pathway that includes *PTEN* and *TSC2* (12–14). The sequences of these genes were then determined by means of Sanger sequencing in a validation set consisting of 58 additional PanNETs and their corresponding normal tissues (Fig. 1, A and B). In total, somatic muta-

tions in *MEN1*, *DAXX*, *ATRX*, *PTEN*, *TSC2*, and *PIK3CA* were identified in 44.1%, 25%, 17.6%, 7.3%, 8.8%, and 1.4% PanNETs, respectively (Table 2).

Of the 30 mutations in *MEN1*, 25 were inactivating mutations [18 insertions or deletions (“indels”), 5 nonsense, and 2 splice-site mutations], whereas five were missense. At least 11 were homozygous; in the others, the presence of “contaminating” DNA from normal cells made it difficult to reliably distinguish heterozygous from homozygous changes. *MEN1* encodes menin, a nuclear protein that acts as a scaffold to regulate gene transcription by coordinating chromatin remodeling. It is an essential component of the MLL SET1-like histone methyltransferase (HMT) complex (15–19). Overall, *MEN1* was mutated in 30 of the 68 PanNETs used in the discovery and validation sets combined.

DAXX and *ATRX* were mutated in 17 and 12 PanNETs, respectively. No tumor with a mutation in *DAXX* had a mutation in *ATRX*, which is consistent with their presumptive function within the same pathway. Overall, 29 of 68 PanNETs (42.6%) had a mutation in this pathway. There were 11 indels and four nonsense mutations in *DAXX* and six indels and three nonsense mutations in *ATRX*. The three *ATRX* missense mutations were within the conserved helicase

domain, whereas the *DAXX* missense mutations were nonconserved changes. Five *DAXX* and four *ATRX* mutations were homozygous, indicating loss of the other allele. The high ratio of inactivating-to-missense mutations in both genes establishes them as PanNET tumor suppressor genes. Loss of immunolabeling for *DAXX* and *ATRX* correlated with mutation of the respective gene (fig. S1, A and B, and table S5). From these data, we hypothesize that both copies of *DAXX* are generally inactivated, one through mutation and the other either through loss of the nonmutated allele or epigenetic silencing. We also hypothesize that both copies of *ATRX* are inactivated, one through mutation and the other through chromosome X inactivation. Recently, it has been shown that *DAXX* is an H3.3-specific histone chaperone (20). *ATRX* encodes a protein that at the amino-terminus has an ADD (*ATRX*-DNMT3L-DNMT3L) domain and a carboxy-terminal helicase domain. Almost all missense disease-causing mutations are within these two domains (21). *DAXX* and *ATRX* interact, and both are required for H3.3 incorporation at the telomeres; *ATRX* is also required for suppression of telomeric repeat-containing RNA expression (22–24). *ATRX* was recently shown to target CpG islands and G-rich tandem repeats (25), which exist close to telomeric regions.

We identified five *PTEN* mutations, two indels and three missense; six *TSC2* mutations, one indel, one nonsense, and four missense; and one *PIK3CA* missense mutation. Previously published expression analyses have indicated that the expression of genes in the mTOR pathway is altered in most PanNETs (26, 27). Our data suggest that, at least at the genetic level, only a subset of PanNETs have alterations of this pathway. This finding may have direct clinical application through prioritization of patients for therapy with mTOR pathway inhibitors. Everolimus [also called Afinitor, RAD-001, and 40-O-(hydroxyethyl)-rapamycin] has been shown to increase progression-free survival in a subset of PanNET patients with advanced disease (28). If the mutational status of genes coding for proteins in the mTOR pathway predicts clinical response to mTOR inhibitors, it should be possible to select patients who would benefit most from an mTOR inhibitor through analysis of these genes in patients' tumors (29, 30).

All 68 tumors evaluated in this study were from patients undergoing aggressive intervention (table S6) and included patients undergoing curative resection as well as those with metastatic disease. Mutations in *MEN1*, *DAXX/ATRX*, or the combination of both *MEN1* and *DAXX/ATRX* were associated with prolonged survival relative to those patients whose tumors lacked these mutations (Fig. 1, C and D, and table S7). This was particularly evident in patients with metastatic disease and with mutations in both *MEN1* and *DAXX/ATRX*: 100% of patients with PanNETs that had these mutations survived at least 10 years,

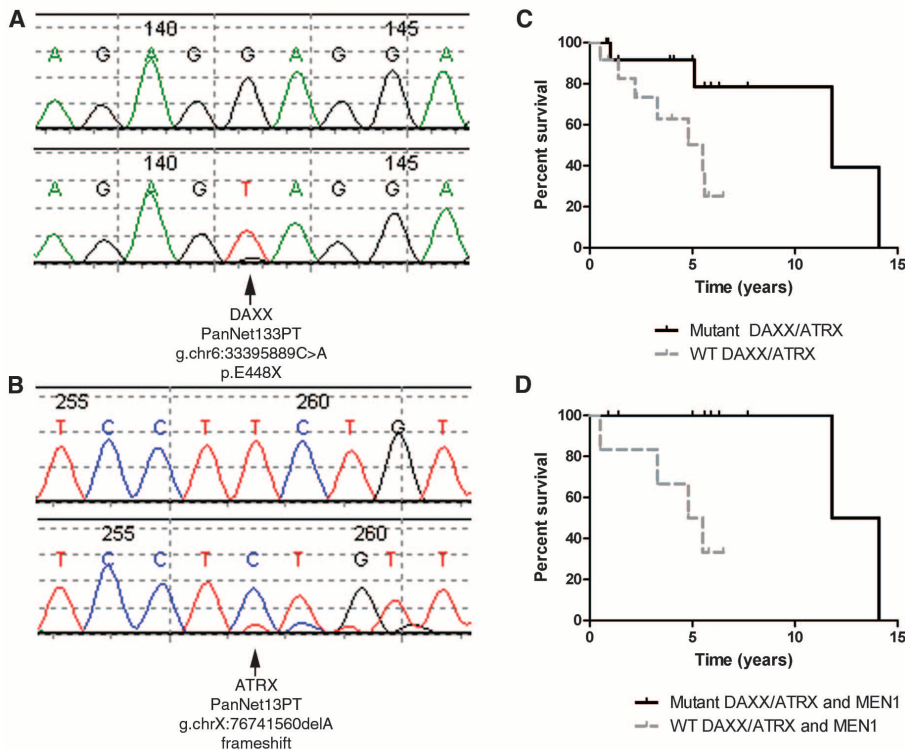


Fig. 1. (A and B) Examples of traces showing mutations in DNA isolated from cancer cells [(A) and (B), bottom] but not from normal cells of the same patient [(A) and (B), top]. (C and D) Kaplan-Meier plots of overall survival of patients with metastatic PanNETs. (C) Fifteen patients with a *DAXX* or *ATRX* gene mutation versus 12 patients in whom both genes were wild type (WT) [hazard ratio 0.22, 95% confidence interval (CI) 0.06 to 0.84, $P = 0.03$]. (D) Nine patients with mutations in *MEN1* as well as either *DAXX* or *ATRX* versus six patients in which all three genes were WT (hazard ratio 0.07, 95% CI 0.009 to 0.53, $P = 0.01$). All types of mutations in these genes were included in the analysis.

whereas over 60% of the patients without these mutations died within 5 years of diagnosis (Fig. 1D). One possible explanation for the difference in survival is that mutations in *MEN1* and *DAXX/ATRX* identify a biologically specific subgroup of PanNETs.

Whole-exome sequencing of pancreatic neuroendocrine tumors has led to the identification of previously unknown tumor suppressor genes and illuminated the genetic differences between the two major neoplasms of the pancreas. The mutations may serve to aid prognosis and provide a way to prioritize patients for therapy with mTOR inhibitors.

References and Notes

- R. H. Hruban, M. B. Pitman, D. S. Klimstra, *Tumors of the Pancreas, Atlas of Tumor Pathology* (American Registry of Pathology and Armed Forces Institute of Pathology, Washington, DC, ed. 4, 2007).
- M. Fredrich, A. Reisch, R. B. Illing, *Exp. Brain Res.* **195**, 241 (2009).
- S. Ekeblad, B. Skogseid, K. Dunder, K. Oberg, B. Eriksson, *Clin. Cancer Res.* **14**, 7798 (2008).
- P. Francalanci et al., *Am. J. Surg. Pathol.* **27**, 1386 (2003).
- V. Corbo et al., *Endocr. Relat. Cancer* **17**, 771 (2010).
- P. Capelli et al., *Arch. Pathol. Lab. Med.* **133**, 350 (2009).
- D. C. Chung et al., *Cancer Res.* **58**, 3706 (1998).
- G. Florida et al., *Cancer Genet. Cytogenet.* **156**, 23 (2005).
- W. Hu et al., *Genes Cancer* **1**, 360 (2010).
- Materials and methods are available as supporting material on Science Online.
- S. Jones et al., *Science* **321**, 1801 (2008).
- D. W. Parsons et al., *Nature* **436**, 792 (2005).
- D. A. Guertin, D. M. Sabatini, *Cancer Cell* **12**, 9 (2007).
- L. J. Shaw, L. C. Cantley, *Nature* **441**, 424 (2006).
- C. M. Hughes et al., *Mol. Cell* **13**, 587 (2004).
- A. Yokoyama et al., *Mol. Cell. Biol.* **24**, 5639 (2004).
- J. Grembecka, A. M. Belcher, T. Hartley, T. Cierpicki, *J. Biol. Chem.* **285**, 40690 (2010).
- H. Kim, J. E. Lee, E. J. Cho, J. O. Liu, H. D. Youn, *Cancer Res.* **63**, 6135 (2003).
- S. K. Agarwal et al., *Cell* **96**, 143 (1999).
- P. W. Lewis, S. J. Elsaesser, K. M. Noh, S. C. Stadler, C. D. Allis, *Proc. Natl. Acad. Sci. U.S.A.* **107**, 14075 (2010).
- R. J. Gibbons et al., *Hum. Mutat.* **29**, 796 (2008).
- P. Drané, K. Ouararhni, A. Depaux, M. Shuaib, A. Hamiche, *Genes Dev.* **24**, 1253 (2010).
- A. D. Goldberg et al., *Cell* **140**, 678 (2010).
- L. H. Wong et al., *Genome Res.* **20**, 351 (2010).
- M. J. Law et al., *Cell* **143**, 367 (2010).
- E. Missaglia et al., *J. Clin. Oncol.* **28**, 245 (2010).
- A. Perren et al., *Am. J. Pathol.* **157**, 1097 (2000).
- J. C. Yao et al., *Ann. Oncol.* **21** (suppl. 8), viii4 (2010).
- P. Liu, H. Cheng, T. M. Roberts, J. J. Zhao, *Nat. Rev. Drug Discov.* **8**, 627 (2009).
- D. A. Krueger et al., *N. Engl. J. Med.* **363**, 1801 (2010).
- We thank M. Whalen for expert technical assistance. This work was supported by a research grant from the Caring for Carcinoid Foundation, by the Lustgarten Foundation for Pancreatic Cancer Research, the Sol Goldman

Pancreatic Cancer Research Center, the Joseph L. Rabinowitz Fund for Pancreatic Cancer Research, the Virginia and D. K. Ludwig Fund for Cancer Research, the Raymond and Beverly Sackler Research Foundation, the American Association for Cancer Research Stand Up To Cancer–Dream Team Translational Cancer Research Grant, and by National Institutes of Health grants CA121113, P50CA062924, P01CA134292, and R01CA113669. N.P. B.V., L.D., V.E.V., and K.W.K. are members of the Scientific Advisory Board of Inostics, a company that is developing technologies for the molecular diagnosis of cancer. N.P. B.V., L.D., V.E.V., and K.W.K. are co-founders of Inostics and Personal Genome Diagnostics and are members of their Scientific Advisory Boards. The authors are entitled to a share of the royalties received by the university on sales of products related to genes described in this manuscript. N.P., B.V., K.W.K., L.A.D., and V.E.V. own Inostics and Personal Genome Diagnostics stock, which is subject to certain restrictions under university policy. The terms of these arrangements are managed by Johns Hopkins University in accordance with its conflict-of-interest policies. D.S.K. is a paid advisor for Novartis, which produces drugs for treatment of neuroendocrine tumors.

Supporting Online Material

www.sciencemag.org/cgi/content/full/science.1200609/DC1

Materials and Methods

Fig. S1

Tables S1 to S8

References

18 November 2010; accepted 10 January 2011

Published online 20 January 2011;

10.1126/science.1200609

Different B Cell Populations Mediate Early and Late Memory During an Endogenous Immune Response

Kathryn A. Pape,¹ Justin J. Taylor,¹ Robert W. Maul,² Patricia J. Gearhart,^{2*} Marc K. Jenkins^{1†}

Memory B cells formed in response to microbial antigens provide immunity to later infections; however, the inability to detect rare endogenous antigen-specific cells limits current understanding of this process. Using an antigen-based technique to enrich these cells, we found that immunization with a model protein generated B memory cells that expressed isotype-switched immunoglobulins (swlg) or retained IgM. The more numerous IgM⁺ cells were longer lived than the swlg⁺ cells. However, swlg⁺ memory cells dominated the secondary response because of the capacity to become activated in the presence of neutralizing serum immunoglobulin. Thus, we propose that memory relies on swlg⁺ cells until they disappear and serum immunoglobulin falls to a low level, in which case memory resides with durable IgM⁺ reserves.

Memory B cells are generated during the primary immune response to foreign antigens. This process is initiated when naïve B cells expressing surface immunoglobulin (Ig) bind the antigen in secondary lymphoid organs, receive signals from helper T cells, and proliferate (1). This proliferation produces short-lived immunoglobulin-secreting plasmablasts and germinal center cells, many of which switch their immunoglobulin constant region from IgM to IgG, IgA, or IgE and acquire somatic mutations

in the variable region (1–3). Cells that acquire immunoglobulin mutations that improve antigen binding gain a survival advantage and emerge from the germinal center reaction as long-lived surface-switched immunoglobulin (swIg)⁺ memory cells, or surface Ig⁺ plasma cells that maintain serum immunoglobulin levels (4). After subsequent exposure to antigen, the memory cells proliferate rapidly and generate plasmablasts, which boost the amount of antigen-specific immunoglobulin in the serum to aid in antigen clearance

(1, 4). There is, however, evidence for the existence of IgM⁺ memory B cells that have or have not passed through germinal centers or undergone somatic mutation (5).

Recently, genetic labeling of B cells that expressed activation-induced cytidine deaminase (AID), which is required for isotype switching and somatic mutation (6), suggested that IgM⁺ memory cells make up part of the memory B cell pool in mice (7). Whether these cells were antigen-specific was not addressed. Thus, the relative contribution of IgM⁺ B cells—especially those that may not express AID—to the antigen-specific memory pool remains unclear.

We sought to gain a comprehensive view of all memory B cells in normal mice by tracing the fate of antigen-specific precursors throughout the primary immune response on the basis of antigen-specificity alone without the complications related to the use of immunoglobulin transgenic mice (8–10). Phycoerythrin (PE) and allophycocyanin were chosen as model foreign antigens because their fluorescent properties

¹Department of Microbiology, Center for Immunology, University of Minnesota Medical School, Minneapolis, MN 55455, USA. ²Laboratory of Molecular Gerontology, National Institute on Aging, National Institutes of Health, Baltimore, MD 21224, USA.

*Present address: Laboratory of Molecular Biology and Immunology, National Institute on Aging, National Institutes of Health, Baltimore, MD 21224, USA.

†To whom correspondence should be addressed. E-mail: jenki002@umn.edu